Journal Pre-proof

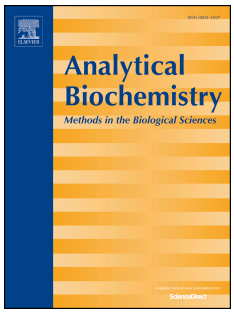

Label-free liquid crystal-based biosensor for detection of dopamine using DNA aptamer as recognition probe

Duy Khiem Nguyen, Chang-Hyun Jang

PII: S0003-2697(20)30339-0

DOI: https://doi.org/10.1016/j.ab.2020.113807

Reference: YABIO 113807

To appear in: *Analytical Biochemistry*

Received Date: 14 February 2020

Revised Date: 25 May 2020

Accepted Date: 27 May 2020

Please cite this article as: D.K. Nguyen, C.-H. Jang, Label-free liquid crystal-based biosensor for detection of dopamine using DNA aptamer as recognition probe, *Analytical Biochemistry*, https://doi.org/10.1016/j.ab.2020.113807.

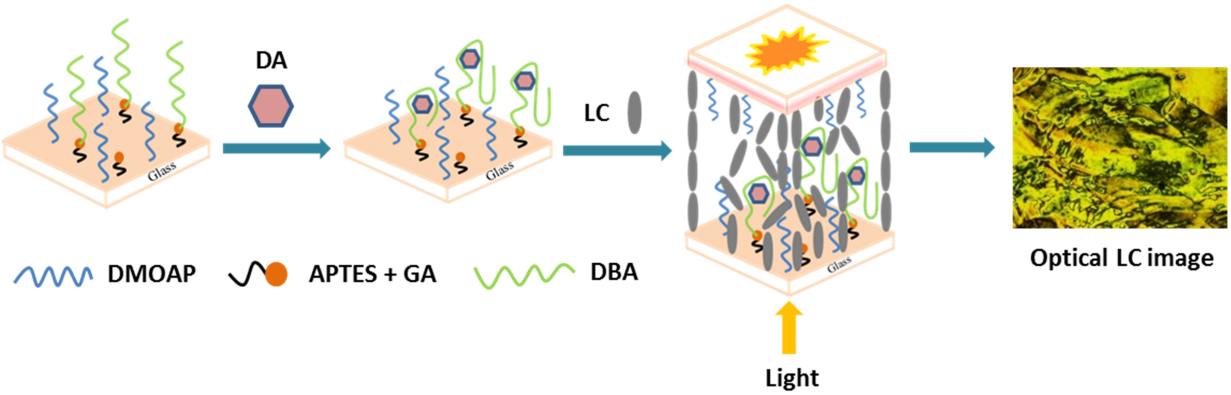

Label-free liquid crystal-based biosensor for detection of dopamine using DNA aptamer as recognition probe

Duy Khiem Nguyen[1], and Chang-Hyun Jang[1,] *

[1]Department of Chemistry, Gachon University, Seongnam-daero 1342, Sujeong-gu, Seongnam-si, Gyeonggi-do 13120, Republic of Korea.

*Corresponding author: Tel. +82-31-750-8555; fax: +82 31 750 8774

E-mail address: chjang4u@gachon.ac.kr (C.-H. Jang)

Abstract

We present a label-free liquid crystal-based biosensor for the detection of dopamine (DA) in aqueous solutions using dopamine-binding aptamers (DBA) as recognition elements. In this system, the dimethyloctadecyl [3-(trimethoxysilyl) propyl] ammonium chloride (DMOAP) self-assembled monolayers immobilized on glass slides support the long alkyl chains that keep the liquid crystal (LC) molecules in a homeotropic orientation. Glutaraldehyde (GA) is used as a cross-linker to immobilize DBA onto the surface of glass slides. The specific binding of DA and DBA disrupts the homeotropic orientation of LCs, thereby inducing a change in the orientation from homeotropic to a random alignment. This orientation change can be converted and visualized simply as a transition from a dark optical LC image to a brighter image under a polarized optical microscope (POM), enabling the detection of DA. The developed LC-based aptasensor shows a good linear optical response towards DA in the very wide range of 1 pM to 10 µM (0.19 pg/ml to 1.9 µg/ml) and having a very low detection limit of 10 pM (~1.9 pg/ml). The proposed LC-based aptamer sensing method offers a simple, rapid, highly sensitive and selective, and a label-free method for the detection of dopamine in aqueous solutions.

Keywords: Liquid crystals; LC-based aptasensors; dopamine; dopamine-binding aptamer

1. Introduction

Dopamine (DA), one of the most essential neurotransmitters in the central and peripheral nervous system, has a strong influence on the control of the feeding, learning, and experiencing pleasure and satisfaction in the brain [1-3]. It also regulates the human addictions, emotions, motivation, movements, and neurocognition [1,4]. An imbalance in the DA concentration in the brain is associated with various neural diseases [5,6]. The depletion of DA may cause Parkinson's disease (PD) and attention deficit hyperactivity disorder (ADHD). On the contrary, elevated levels of DA often cause euphoria, schizophrenia, a state of pleasurable, or may indicate the presence of dopamine-producing neuroendocrine tumors, i.e., paragangliomas [7-9]. For example, the plasma level of DA in healthy adults ranges around 0.1 nmol/l on an average [10], and those with head and neck paragangliomas ranges up to 6.05 nmol/l [11]. Moreover, dopamine is exploited as an animal growth promoter to help the stocks build muscle rather than fat; and ingesting animal products containing residual DA may cause food poisoning [7]. Owing to its important role in health and disease, development of an analytical method for the precise detection of DA levels with high sensitivity and selectivity bears a huge significance in basic pathophysiology and drug development studies, as well as in monitoring, diagnosis, and treatment of patients.

Until now, several methods have been developed for DA determination, such as high performance liquid chromatography (HPLC) [12], liquid chromatography coupled with mass spectrometry (LC-MS) [13,14], colorimetry [4,15], fluorescence [16], and electrochemistry [17]. However, chromatographic methods call for expensive equipment, professional operation, and time-consuming procedures. In contrast, colorimetric methods do not need any expensive equipment and the results can be directly visualized. However, they are accompanied by drawbacks such as low sensitivity, complicated procedures, and background signal interference in the sample matrix [4]. Fluorescent sensors have attracted much attention due to their high sensitivity, quick response, low background interference, and easy operation [12,18,19]. These methods are mainly based on utilization of fluorescent nanoparticles (NPs) such as quantum dots, metal NPs, or silica NPs as probes. Nevertheless, the synthesis procedures of fluorescent NPs are relatively complicated and time-consuming [7]. The electrochemical method is efficient for the determination of highly electroactive dopamine due to its rapid response, high accuracy, high sensitivity, and low cost [17,20-22]. However, this method has limited selectivity because of the interference of physiologically

coexisting ascorbic acid and uric acid, both of which are also electroactive and possess similar oxidation/reduction potentials [7,23].

The aptamer technology can resolve problems of limited selectivity because of its excellent recognition and binding ability to the target molecules, and thereby, is expected to eliminate the interference caused by other molecules. It is well-known that aptamers are artificial, short, single-stranded oligonucleotides (ssDNA or ssRNA) selected from random-sequence nucleic acid libraries using the systematic evolution of ligands with exponential enrichment (SELEX) process [24,25]. They possess the ability to recognize various target molecules, such as drugs [26], proteins [27-29], small molecules [30], and even cancer cells with high affinity and specificity [31]. Due to their distinctive properties, including small size, simple synthesis and modification, cost-effectiveness, good stability, and wide applicability, the aptamers have been widely employed as recognition elements for biosensors using colorimetric [4,27], fluorescent [7], electrochemical [32], electrochemiluminescent [33], piezoelectric [34], and LC-based sensing methods [35,36]. Among them, the LC-based sensors have attracted the greatest interest because of their excellent sensitivity, rapid response, simplicity, and low cost [32,35]. Moreover, this sensing method does not need any additional labeling step, complicated procedures, and expensive instrumentation [37-39]. The combination of highly sensitive LC-based sensing method and highly specific aptamer technology provides novel strategies for the effective detection of target molecules. Therefore, LC-based aptamer sensors have been robustly developed for the detection of various target molecules, such as interferon-γ [35], bisphenol A [36], thrombin [40], and heavy metal Ions [41,42].

In the present study, we developed a novel optical LC-based aptasensor for the determination of DA in aqueous solutions using dopamine-binding DNA aptamers (DBA) as recognition elements. The detection principle of this aptasensor is based on the orientation change of the LC molecules caused by the binding of DA molecules to the DBA-immobilized surface. When a DA-containing sample is incubated with the DBA-immobilized surface, the DA is selectively captured by the DBA. Hence, the conformation of DBA shifts from a random coil structure to a rigid tertiary stem–loop structure [4,43], leading to a change in the surface topography of the substrate; this disrupts the vertical orientation of the LC molecules, resulting in a change of optical signals [35,44]. Moreover, the orientation changes of the local LC molecules affect the distribution of the surrounding LC molecules resulting in a certain amplification of optical signals [45]. The orientation transition of the LC molecules

can be readily observed under POM as a transition from dark to bright optical image [35]. Based on this change, DA can be detected selectively and with greater sensitivity. Lower detection limit of 10 pM (~1.9 pg/ml) was obtained while the determination of DA as compared to other reported methods [1,15,46]. In addition, this sensor showed a good selectivity towards DA. Therefore, this label-free optical LC-based aptasensor is undemanding and would be a promising platform for real-time determination of DA with high selectivity and sensitivity not only in aqueous solution but also in real clinical samples.

2. Materials and Methods

2.1 Materials

Dimethyloctadecyl [3-(trimethoxysilyl) propyl] ammonium chloride (DMOAP, 70%), glutaraldehyde (GA, 50%), (3-aminopropyl) triethoxysilane (APTES, ≥98%), dopamine hydrochloride, pyrocatechol, epinephrine, ethanolamine, and phosphate buffered saline (PBS, pH 7.4) were purchased from Sigma-Aldrich (St. Louis, MO, USA). Nematic liquid crystal 4-cyano-4'-pentylbiphenyl (5CB) was obtained from Tokyo Chemical Industrial Co., Ltd (Tokyo, Japan). The 5'-amino modified 58-mer DNA aptamer specific for dopamine (5'-/5AmMC6/NH_2-GTC TCT G**TG TGC** GCC AGA GAA CAC TGG GGC AGA TAT GGG CCA **GCA CA**G AAT GAG GCC C-3') was synthesized by Mbiotech (Hanam, South Korea). The residues forming the dopamine binding site are bold and underlined. This 58-mer DNA oligomer, i.e., the dopamine targeting aptamer was chosen based on previous studies [4,47]. Hydrogen peroxide (H_2O_2, 30% w/v), sulfuric acid (H_2SO_4, 95%), ethanol, and methanol were purchased from Daejung Chemicals & Metals Co., Ltd (Daejung, South Korea). Micro slide glass was acquired from Matsunami Glass IND., Ltd (Osaka, Japan). Silicon wafer was obtained from Silicon Sense (Nashua, USA). All reagents were used as received without further purification. Deionized (DI) water (18.2 $M\Omega.cm^{-1}$, Milli-Q water purification system, Millipore, Bedford, MA, USA) was used throughout the experiments. Stock solutions of catecholamines were prepared daily in DI water and protected from light.

2.2 Fabrication of optical LC cells

After the glass slides were treated with Piranha solution, most of the organic matters were removed and hydroxyl groups (-OH) were formed on the surface of the glass slides. The substrate membrane

of the LC cells was constructed by using a mixed monolayer of APTES and DMOAP. The alkoxyl groups (C_2H_5O-) in APTES and DMOAP molecules react with the -OH groups leading to a stable grafting of APTES and DMOAP onto the surface of the glass slides. When GA is added, the amino group (-NH_2) in APTES on the surface reacts with the aldehyde group (-CHO) on one end of GA molecule. The aldehyde group on the other end reacts with the amino group in DBA resulting in the immobilization of DBA onto the substrate glass slides (Fig. S1). The optical LC cells were made by pairing the covering glass slides decorated with 0.4% DMOAP and modified substrate glass slides face to face and then held together with small blinder clips. A thin polyester film (thickness = 10 μm) was used to produce a gap between the two glass slides.

2.2.1 Piranha treatment of glass slide

The micro glass slides were cut into sizes of 2.5 cm × 1 cm and immersed in the freshly prepared Piranha solution (H_2SO_4/H_2O_2 = 7/3 [v/v]) at 80°C for 1 h in a nitrogen-rich a tmosphere. After cooling, the Piranha-treated glass slides were rinsed turn-wise with DI water, ethanol, and methanol to remove the residual acid, followed by drying under nitrogen flow, and heating in an oven at 120°C overnight. Hydroxyl groups were formed on the surface of the glass slides after treatment.

2.2.2 Preparation of covering glass slide

The covering (upper) glass slide was modified with DMOAP. The Piranha-treated glass slides were soaked in an aqueous solution containing 0.4% (v/v) of DMOAP at room temperature for 30 min, rinsed several times with DI water, dried with nitrogen flow, and heated at 120°C for 1 h.

2.2.3 Preparation of lower glass slide

2.2.3.1 Preparation of GA-modified substrate glass slide

The substrate glass slide was firstly decorated with the mixed APTES/DMOAP. The Piranha-treated glass slides were immersed in an ethanol solution containing a mixture of APTES (0.2%, v/v) and DMOAP (0.2%, v/v) at 80°C for 1 h (Fig. S1 (a)). A fter washing with ethanol and DI water for several times, the glass slides were dried under nitrogen flow and heated at 120°C for 1 h. Subsequently, the APTES/DMOAP-modified glass slides were immersed in an aqueous solution containing GA (0.1%, v/v) at room temperature for 30 min, followed by washing with DI water. The slides were then dried in a nitrogen stream, and stored at 4°C until further use (Fig. S1 (b)).

2.2.3.2 Immobilization of DBA onto the substrate glass slide

The DBA solutions with various concentrations were prepared by diluting a 100 µM DBA stock solution with 10 mM PBS buffer (pH = 7.4, 138 mM NaCl, 2.7 mM KCl). A volume of 10 µl of DBA solution at each concentration was added dropwise to the surface of GA-modified substrate glass slides, and then incubated at 37° C for 1 h in an o ven (Fig. S1 (c)). After cooling, the substrate glass slides were washed successively with 10 mM PBS buffer (pH = 7.4) and DI water several times to remove the unbinding DBA, and then dried in a nitrogen stream. To block the unreacted aldehyde groups, the DBA-immobilized substrate glass slides were immersed in 20 mM aqueous ethanolamine solution at room temperature for 30 min. After reaction, the substrate glass slides were washed with DI water, dried with nitrogen flow, and stored at 4° C until further use.

2.2.3.3 Specific binding of DBA and DA

Stock solution of DA was freshly prepared on the day of use in DI water and protected from light. Various concentrations of DA solution were prepared by diluting a 1 mM dopamine stock solution with DI water. A volume of 10 µl of DA solution at each concentration was poured on the DBA-immobilized substrate glass slides and incubated at 37° C for 1 h, followed by washing with DI water to remove unbound agents, and drying under a stream of nitrogen. In order to verify the specificity of the fabricated LC aptasensor, molecules with similar structures such as pyrocatechol and epinephrine were tested under similar conditions.

2.2.4 Fabrication of optical LC cells.

The optical LC cells were made by pairing the covering glass slides coated with 0.4% DMOAP and decorated substrate glass slides (lower glass slide) face to face and then held together with small blinder clips (Fig. 1A). A thin polyester film (thickness = 10 µm) was used to produce a gap between two glass slides. 5CB was heated to ~40° C (isotrop ic phase of 5CB) using a heat gun and injected into the gap between the glass slides using a micropipette. Finally, the optical LC cells were slowly cooled to 25° C (nematic phase of 5 CB) prior to ch aracterization.

2.3 Characterization

A polarized optical microscope (POM, Eclipse LV100 POL, Nikon, Tokyo, Japan), mounted with a digital camera (DS-2Mv, Nikon, Tokyo, Japan) was used to capture images of the LC optical responses. All images were observed using 10× objective lenses at a resolution of 2560 × 1920 pixels. The gray-scale of all optical images was calculated using Adobe Photoshop CC2018 software. Surface morphology of all samples was examined using an atomic force microscope (AFM, Nanoscope IIIa, Veeco, Santa Barbara, CA, USA). The AFM images were captured in the tapping mode with a scan rate of 1 Hz, 512 samples per line, and scanning scope of 1 μm × 1 μm. The change in the root mean square (RMS) roughness was measured after each step of modification. The optical thickness of the samples at each modification step was characterized using an ellipsometer (Elli-SE(UV)-FM8, Ellipso technology, Suwon, South Korea) equipped with halogen and deuterium lamps as light sources (wavelengths: 380~1100 nm). The specimens for AFM and optical thickness measurement were prepared using flat silicon wafers instead of micro slide glass during chemical modification while the reaction conditions remained unaltered.

3. Results and discussion

3.1. Fabrication and principle of optical LC-based aptasensor

The fabrication of optical LC-based aptasensor for DA detection is illustrated in Fig. 1A. The Piranha-treated glass slide (Fig. 1A (a)) was modified with DMOAP 0.4% (v/v) and used as covering part (Fig. 1A (b)). A mixture of APTES/DMOAP was chemically fixed on the surface of another Piranha-treated glass slide not only to provide a long chain of DMOAP for vertical alignment of LC molecules, but also to provide an active amino group in APTES for further grafting of GA (Fig. 1A (c)). The DBA was then immobilized on the surface of glass slides via chemical reaction of amino group in DBA with the aldehyde group from GA molecules to form stable imine bonds (Fig. 1A (d)).

It is well known that the orientation changes in LCs are closely related to changes in the topographical surface in contact with the LC molecules. Thus, in the absence of DA, the conformation of the aptamer remains in a random coil structure (Fig. 1B (g)) so that it does not affect the alignment of the LC molecules resulting in uniform dark POM images (Fig. 1B (k)). When DA is present, it specifically interacts with DBA to form an “aptamer-target” complex with a rigid tertiary structure (Fig. 1B (h)) [43]. The large complex size causes a change in the surface topography of substrate and disrupts the orientation of the LC molecules from vertical to random/tilted orientation (Fig. 1B (j)),

yielding bright POM images (Fig. 1B (l)). The transition from dark to bright images was readily observed under POM and visualized with a naked eye, allowing the qualitative examination of the presence or the absence of DA on the surface. Different degrees in the surface modification in turn induced different degrees in the orientation change of the corresponding LC molecules, finally resulting in differential extent in the brightness of the obtained POM images. Based on this, the DA content in the samples can be examined quantitatively.

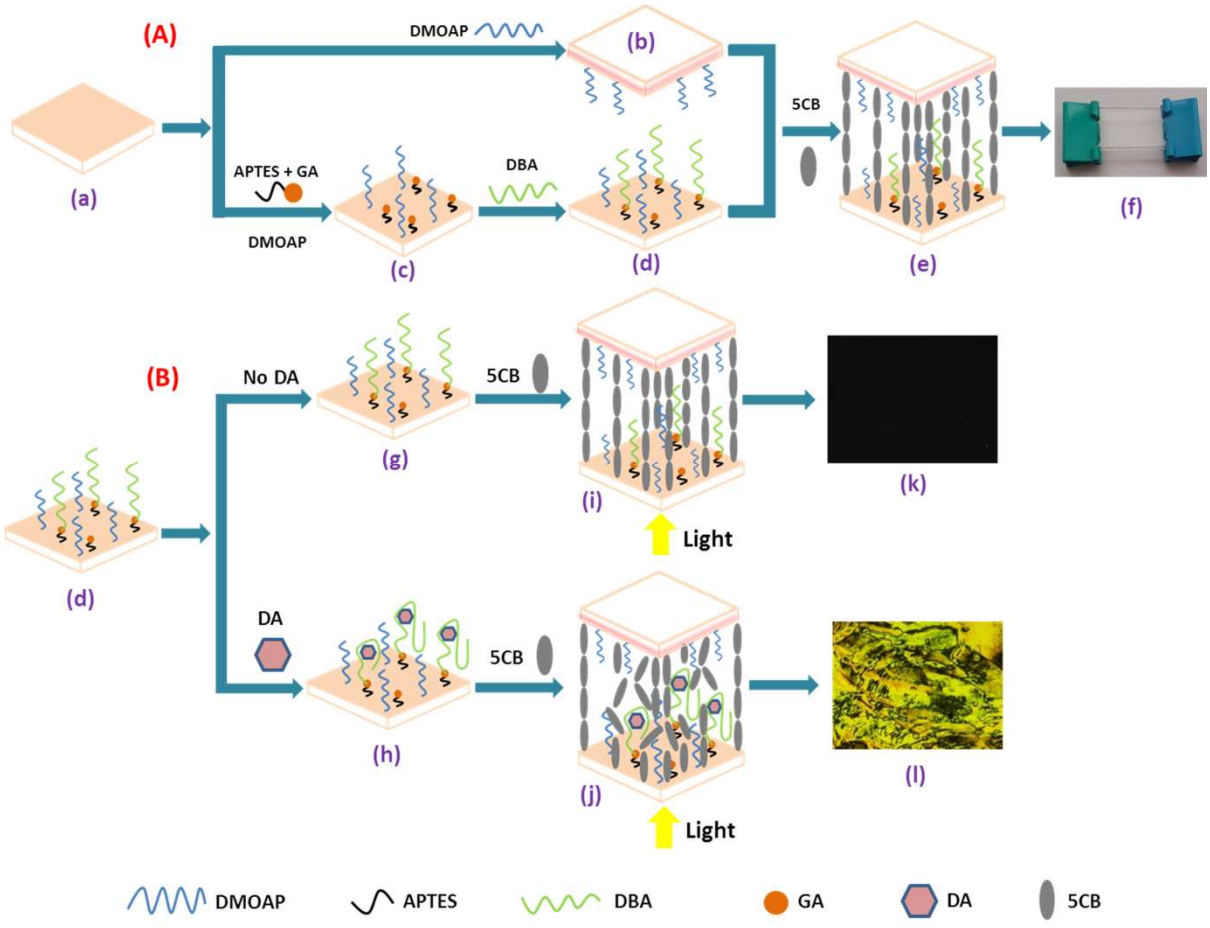

Fig. 1 Illustration of preparation steps for optical cells (A), and detection strategy of dopamine (B). (a) Piranha-treated glass; (b) Covering glass; (c) DMOAP/APTES/GA-functionalized glass; (d) DBA-immobilized glass; (e) Structure diagram of an LC cell; (f) The physical picture of an LC cell; (g) Glass substrate after incubation with PBS (pH = 7.4); (h) After binding with DA, the conformation of DBA changes to rigid tertiary stem–loop structures; (i) vertical alignment of LC 5CB molecules in the optical cells in the absence of DA; (j) specific binding of DBA to DA disrupts the vertical orientation of LC 5CB

molecules in the optical cells; (k) POM image in the absence of DA; and (l) POM image in the presence of DA

3.2 Optimization of sensor fabrication conditions

As mentioned, the surface modification of LC cells has a great influence on the background signals. Thus, we first investigated the optimal ratio between APTES and DMOAP. The Piranha-treated glass slide was immersed in mixed APTES/DMOAP ethanol solution prepared in various ratios, while the DMOAP concentration was fixed at 0.2% (v/v). The LC cells were then fabricated and examined using a POM. As shown in Fig. S2 (a), bright optical image of LC cells was observed at the APTES/DMOAP ratio of 5:1, corresponding to a random orientation of LC molecules. However, when the APTES/DMOAP ratio was reduced to 3:1, a number of bright spots were noted in the optical LC image (Fig. S2 (b)). Lastly, a uniform dark background was obtained when the APTES/DMOAP ratio was reduced to 1:1 corresponding to a perpendicular orientation of LC molecules (Fig. S2 (c)). Thus, the APTES/DMOAP ratio of 1:1 was employed in the further experiments.

The APTES/DMOAP-modified glass slides prepared were then incubated in the GA aqueous solutions with different concentrations, and the concentration of GA was optimized. As shown in Fig. S3 (a), a bright optical image was obtained as the modified glass slides were incubated in 1% (v/v) GA solution, corresponding to a random orientation of the LC molecules. Figures S3 (b) and S3 (c) show that the dark optical LC images were observed when the GA concentrations were equal to or less than 0.1% (v/v), corresponding to a vertical alignment of the LC molecules. Therefore, to avoid background signal interference and to ensure a sufficient number of aldehyde functional groups for the next immobilization of DBA, an optimized GA concentration of 0.1% (v/v) was employed in the subsequent experiments.

Since the surface topography is closely related to the concentration of surface-immobilized aptamers, it is necessary to investigate the optimal concentration of DBA that would be required to maintain the homeotropic orientation of the LC molecules and to improve the signal-to-background contrast. Figure 2 shows the optical images of LC cells fabricated from the GA-modified glass slides incubated in DBA solutions with variable concentrations. The bright areas in the optical images lessened with the reducing concentrations of DBA. As shown in Figs. 2a-2c, bright optical images were obtained when the concentrations of DBA were greater than 100 nM, corresponding to a random

orientation of the LC molecules. This is attributed to high concentration of aptamer, causing the changes in the surface topography leading to an alignment disturbance of the LC molecules. Dark optical images were observed as the DBA concentrations were equal to or less than 10 nM (Figs. 2d and 2e), corresponding to a homeotropic orientation of the LC molecules. Thus, the aptamer concentration of 10 nM was chosne not only to keep the optical imaging background dark but also to maximize the aptamer concentration for enhancing the sensitivity of the aptasensor.

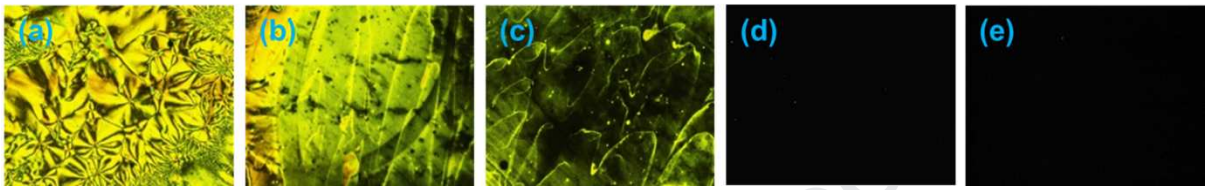

Fig. 2 Optical images of LC cells with 5CB under POM in different concentrations of DBA: (a) 10 μM, (b) 1 μM, (c) 100 nM, (d) 10 nM, and (e) 1 nM in PBS (pH 7.4). The width of each image was 1.25 mm

3.3 Detection of DA by optical LC-based aptasensor

To verify the possibility of detecting DA using this developed LC-based aptasensor, DBA-immobilized glass slides were incubated in serial dilutions of DA aqueous solutions ranging from 1 pM to 10 μM. After incubation, the binding of DA to the surface was detected by monitoring the optical responses of LCs under POM. We hypothesized that the homeotropic arrangement of LCs would be disrupted after binding of DA to the DBA-immobilized surfaces due to changes in the surface topography caused by the conformational changes in the aptamer, resulting in an acquisition of random arrangement of the LCs. Indeed, as can be seen from Fig. 3, a gradual change from dark optical LC images to the bright ones was observed with increasing concentrations of DA from 1 pM to 10 μM. This demonstrated that the orientation of LC molecules had been changed from homeotropic arrangement to a random arrangement after capturing DA on the DBA-immobilized surfaces.

Since the density of DA molecules bound with DBA-immobilized surface is correlated to the extent of surface topographical changes, a sufficient concentration of DA is required to disrupt the alignment of LC molecules on the surface. Thus, this LC-based aptasensor was applied to determine the minimum concentration of DA that could induce the orientation transition of the LC molecules. As shown in Fig. 3a, a uniform dark optical image was observed under POM when the DBA-immobilized glass slide was incubated with a 1 pM DA solution, indicating that 1 pM DA cannot interfere with the

ordered arrangement of LC molecules. As the concentration of DA increased from 10 pM to 1 µM, a large number of bright spots and obvious interference in the optical images were recorded (Fig. 3b-3g). However, the bright domains did not entirely cover the LC images. An almost completely bright optical image was obtained when the DBA-immobilized glass slide was incubated with a solution containing 10 µM DA (Fig. 3h). These results demonstrate that the developed LC-based aptasensor can be applied to examine the presence of DA in aqueous samples. Moreover, the given results suggest that a minimum concentration of 10 pM DA is required to induce the orientation change of LC molecules from a homeotropic to random orientation visible under POM. Therefore, we determined that the limit of detection (LOD) of this LC-based aptasensor for DA was 10 pM.

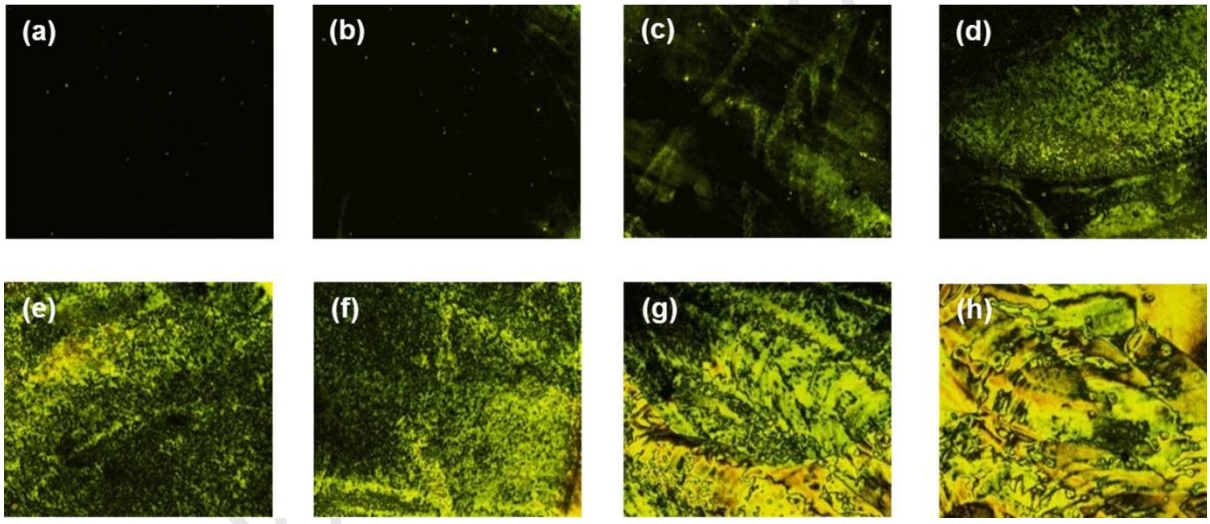

Fig. 3 Optical images of LC cells with 5CB under POM in the presence of different concentrations of Dopamine: (a) 1 pM; (b) 10 pM; (c) 100 pM; (d) 1 nM; (e) 10 nM; (f) 100 nM; (g) 1 µM; and (h) 10 µM. The width of each image was 1.25 mm

3.4 Quantitative analysis of DA concentration

The correlation between the gray-scale intensity of the obtained optical LC images and the concentration of DA was also explored to quantitatively analyze the content of DA in aqueous solutions. The gray-scale intensity of each optical image was calculated using Adobe Photoshop CC2018 software. All quantitative analyses were repeated thrice and the results are presented as mean ± standard deviation (SD). As shown in Fig. 4, the average gray-scale intensity of optical LC image gradually increased as the DA concentration logarithm raised from 1 to 7, corresponding to DA

concentration increase from 1 pM to 10 µM (0.19 pg/ml to 1.9 µg/ml). Good linear relationships of average gray-scale intensity with DA concentration were observed in the concentration range from 1 pM to 10 µM with a high linear correlation coefficient (R^2) of 0.985.

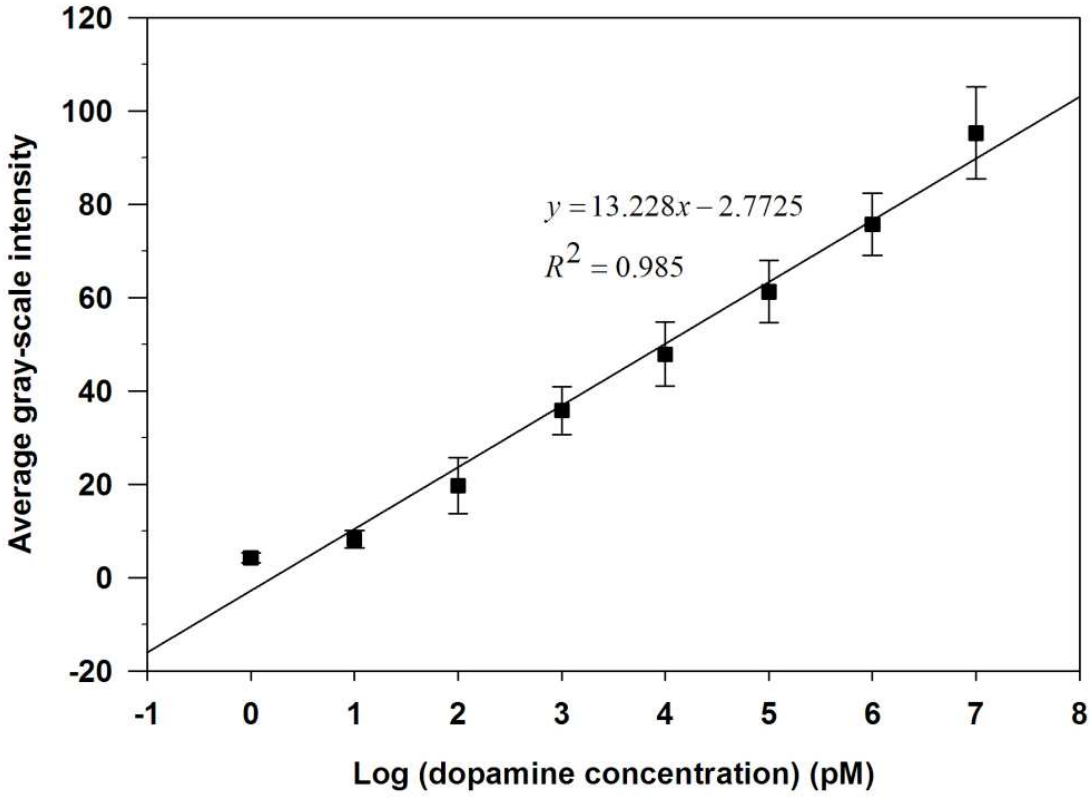

Fig. 4 Relationship between gray-scale intensity of optical LC images and DA concentrations

Using this LC-based aptasensor, DA concentration as low as 10 pM could be successfully detected. The LOD of LC-based aptasensor for DA (10 pM) is considerably lower than that of the previously reported methods (Table 1). Thus, compared to other methods for DA detection, our method offers higher sensitivity, low cost, rapid response and a label-free and easy mode to fabricate without requiring complex processes or instruments.

Table 1 Comparative analysis of the dopamine sensors

Analytical method	Target	Linear range	Detection limit	Reference
RNA-aptamer electrode	Dopamine	–	114 nM	[1]

Colorimetry	Dopamine	0.5–3.8 nM	0.05 nM	[15]
Fluorescence	Dopamine	16.7–47.4 μM	1.41 μM	[16]
Electrochemistry	Dopamine	80–400 μM	9.6 μM	[17]
Aqueous/LC interface	Dopamine	0.3–500 μM	0.3 μM	[46]
Polarized optical microscopy	Dopamine	1 pM–10 μM	0.01 nM	Present study

3.5 Specificity of optical LC-based aptasensor

Beside the sensitivity, the selectivity of the LC-based aptasensor was also investigated by examining the optical response of the LC molecules in the optical cells after incubation of DBA-immobilized surface in pyrocatechol, epinephrine, and PBS buffer (pH 7.4) solutions. Pyrocatechol and epinephrine were selected as interferences because of their structural relatedness (catecholamines), while PBS buffer was used as a control. Pyrocatechol and epinephrine, each at the concentration of 10 μM (same as dopamine) were used to prepare the optical LC cells prior to the visualization of optical images under POM. The optical images for pyrocatechol (Fig. 5b) and epinephrine (Fig. 5c) show a uniformly dark appearance with a few low-brightness spots. These weakly bright spots may be due to some residual unbound molecules that remain in the system following insufficient washing. In case of PBS buffer (pH 7.4), a uniformly dark optical image was observed (Fig. 5d). On the contrary, a bright image was clearly obtained in case of dopamine (Fig. 5a). These findings imply that the above interferences cannot bind to the aptamer-immobilized surface and the LC-based aptasensor has a good selectivity towards DA. The high selectivity of this sensor suggests a great potential for DA detection in analytes with complicated compositions.

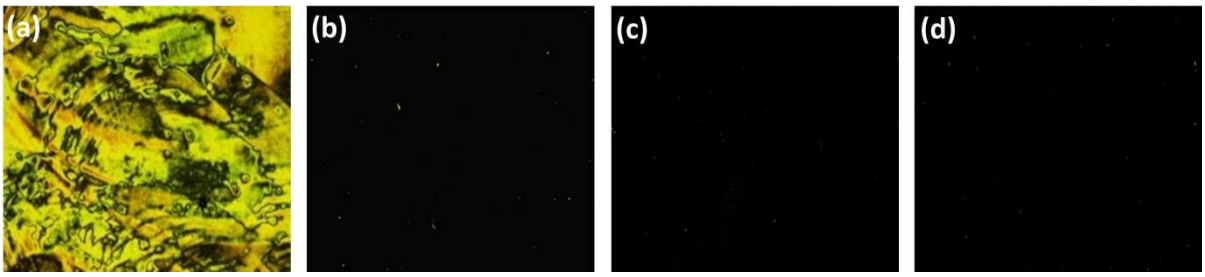

Fig. 5 Optical images of LC cells with 5CB under POM after incubation of aptamer-immobilized surface with (a) 10 μM dopamine; (b) 10 μM pyrocatechol; (c) 10 μM epinephrine; and (d) PBS (pH 7.4). The width of each image was 1.25 mm

3.6 Surface characterization by AFM and ellipsometry

The substrate surface topography was characterized by AFM and ellipsometry to confirm the successful immobilization of different reagents onto the substrate surface. It also confirmed that the binding of dopamine to the aptamer results in the change in surface topography of the substrate, thus leading to the change in optical response of LC molecules in the optical cells. A flat silicon wafer was used as a substrate instead of a glass slide to minimize the background signal in both AFM and ellipsometry.

Figure 6 shows the AFM images of height data on the 5 nm scale. The inset table displays the RMS roughness data. The RMS roughness of samples at each modification step was examined and compared. The APTES/DMOAP-modified surface had an RMS roughness of 0.242 ± 0.045 nm and appeared smooth (Fig. 6a). After modification with GA solution, the RMS roughness slightly increased to 0.324 ± 0.016 nm, probably due to the grating of GA on the surface (Fig. 6b). After further immobilization of the aptamer, the RMS roughness marginally increased to 0.504 ± 0.036 nm while the surface topography remained almost unchanged (Fig. 6c), suggesting that the aptamer was uniformly immobilized on the surface. When the aptamer-immobilized surface was incubated with dopamine, the RMS roughness dramatically increased to 0.943 ± 0.121 nm and the corresponding 3D AFM image showed that the surface topography clearly changed with peaks of variable heights (Fig. 6d). This confirms that the binding of DA to the aptamer-immobilized surface causes changes in surface topography of the substrate, further inducing the orientation transition of LC molecules in the optical cells. The aptamer-immobilized surface was also incubated with pyrocatechol and epinephrine as controls and the 3D AFM images are shown in Fig. 6e and 6f, respectively. Although the concentrations of pyrocatechol and epinephrine used were same as that of dopamine, their RMS roughnesses values were lower and similar to that of an aptamer-modified surface. This result suggests that pyrocatechol and epinephrine were not bound to the aptamer-immobilized surface, resulting in no significant effect on the perpendicularly oriented alignment of LC molecules in the LC cells.

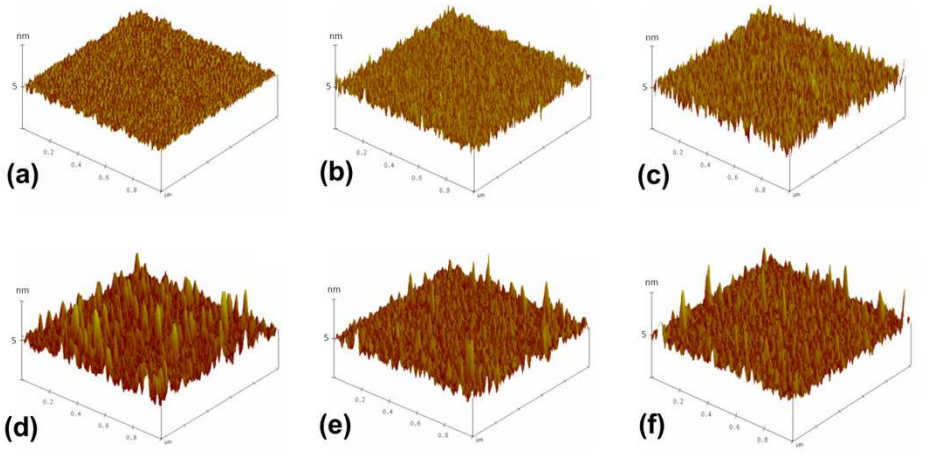

RMS roughness (nm)	
(a)	0.242 ± 0.045
(b)	0.324 ± 0.016
(c)	0.504 ± 0.036
(d)	**0.943 ± 0.121**
(e)	0.511 ± 0.081
(f)	0.510 ± 0.058

Fig. 6 Three-dimensional scanning probe microscope images of the silicon wafer substrates after (a) modification with APTES/DMOAP; (b) grafting with GA; (c) immobilization of the aptamer; and incubation with (d) 10 μM dopamine, (e) 10 μM pyrocatechol, and (f) 10 μM epinephrine; The table on the right shows the RMS roughness data of the respective images

Figure 7 shows the optical thickness of the organic surface layer at each step of the modification obtained by ellipsometry. Herein, the optical thickness was measured using an optical method, therefore it is different from the actual physical thickness. While the optical thicknesses of the APTES/DMOAP-modified surfaces before and after grafting with GA were similar (1.57 ± 0.026 and 1.88 ± 0.031 nm, respectively) (Fig. 7a and 7b), it was slightly increased i.e., 2.93 ± 0.035 nm after the immobilization of the DBA (Fig. 7c). When the DBA-immobilized glass slide was incubated with DA, the optical thickness increased to 3.78 ± 0.056 nm (Fig. 7d). This elevation could be attributed to the interactions of DA and DBA. Similarly, we tested the optical thickness values of surfaces after incubation of DBA-immobilized glass slides with pyrocatechol and epinephrine as controls. The optical thickness values were 2.67 ± 0.019 nm and 2.87 ± 0.07 nm for pyrocatechol and epinephrine, respectively (Fig. 7e and 7f). In this case, the optical thicknesses did not change much as compared to that of aptamer-immobilized surface since the pyrocatechol and epinephrine were not bound to the aptamer-immobilized surfaces. This finding is consistent with the above AFM results. These data substantiate the change in the surface topography of the sensor after modifications and can be used

to explain for the orientation transition of the LC molecules after binding of DA with the aptamer-immobilized surface as well as for the high selectivity of this sensor in the detection of DA.

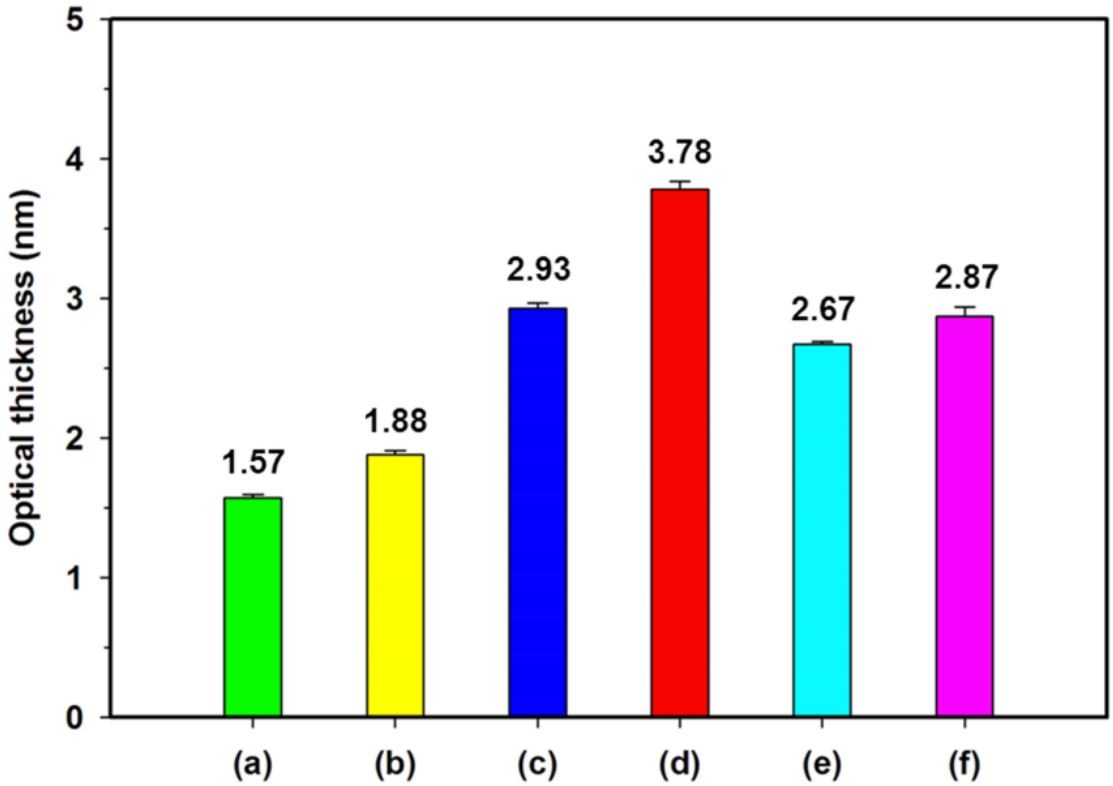

Fig. 7 Optical thickness of the organic surface layer after (a) modification with APTES/DMOAP; (b) grafting with GA; (c) immobilization of the DBA; and incubation with (d) 10 μM dopamine, (e) 10 μM pyrocatechol, and (f) 10 μM epinephrine

4. Conclusions

In summary, we have developed a novel method for the detection of dopamine in aqueous solutions. This process is based on a non-labeled liquid crystal aptamer sensor with a change in liquid crystal orientation from homeotropic to random after binding of dopamine to the aptamer-immobilized surface. This change was readily observed as a transition from a dark optical liquid crystal image to a bright one using a polarized optical microscope. Quantitative analysis was performed and a good linear relationship between average gray-scale values and dopamine concentration was observed in the concentration range from 1 pM to 10 μM. Through this sensing technique, the detection limit of

dopamine could be set as low as 10 pM (~1.9 pg/ml). In addition, surface analysis by AFM and ellipsometry supported that the orientation transition of LC molecules from homeotropic to random alignment was caused by the specific binding of dopamine to the aptamer-immobilized surface. Moreover, the selective investigation demonstrated that this sensor had a good selectivity towards DA. This proposed LC-based aptamer sensing method not only offers a simple, rapid, and label-free method for the detection of dopamine in aqueous solutions with high selectivity and sensitivity, but is also expected to be a promising platform for real-time estimation of dopamine in real clinical samples.

Acknowledgments:

This work was supported by the Basic Science Research Program of the National Research Foundation of Korea (NRF) funded by the Ministry of Education (NRF-2019R1A2C1003862).

Conflict of Interest: The authors declare no conflict of interest.

References

[1] I. Álvarez-Martos, A. Møller, E.E. Ferapontova, Dopamine binding and analysis in undiluted human serum and blood by the RNA-aptamer electrode, ACS Chem. Neurosci. 10 (2019) 1706-1715.

[2] M.A. Kurian, P. Gissen, M. Smith, S.J.R. Heales, P.T. Clayton, The monoamine neurotransmitter disorders: an expanding range of neurological syndromes, Lancet. Neurol. 10 (2011) 721-733.

[3] Z. Anajafi, M. Naseri, S. Marini, C. Espro, D. Iannazzo, S.G. Leonardi, G. Neri, NdFeO3 as a new electrocatalytic material for the electrochemical monitoring of dopamine, Anal. Bioanal. Chem. 411 (2019) 7681–7688.

[4] Y. Zheng, Y. Wang, X. Yang, Aptamer-based colorimetric biosensing of dopamine using unmodified gold nanoparticles, Sens. Actuators B Chem. 156 (2011) 95–99.

[5] S.E. Hyman, R.C. Malenka, Addiction and the brain: the neurobiology of compulsion and its persistence, Nat. Rev. Neurosci. 2 (2001) 695–703.

[6] B.J. Venton, R.M. Wightman, Psychoanalytical Electrochemistry: Dopamine and Behavior, Anal. Chem. 75 (2003) 414 A–421 A.

[7] J. Xu, Y. Li, L. Wang, Y. Huang, D. Liu, R. Sun, J. Luo, C. Sun, A facile aptamer-based sensing strategy for dopamine through the fluorescence resonance energy transfer between rhodamine B and gold nanoparticles, Dyes Pigments. 123 (2015) 55–63.

[8] G. Eisenhofer, D.S. Goldstein, P. Sullivan, G. Csako, F.M. Brouwers, E.W. Lai, K.T. Adams, and K. Pacak, Biochemical and clinical manifestations of dopamine-producing paragangliomas: utility of plasma methoxytyramine, J. Clin. Endocrinol. Metab. 90 (2005) 2068−2075.

[9] S.D. Iversen, L.L. Iversen, Dopamine: 50 years in perspective, Trends. Neurosci. 30 (2007) 188−193.

[10] D.S. Goldstein, G. Eisenhofer, I.J. Kopin, Sources and significance of plasma levels of catechols and their metabolites humans, J. Pharmacol. Exp. Ther. 305 (2003) 800−811.

[11] A.N.A. Van Der Horst-Schrivers, T.E. Osinga, I.P. Kema, B.F.A.M. Van Der Laan, R.P.F. Dullaart, Dopamine excess in patients with head and neck paragangliomas, Anticancer Res. 30 (2010) 5153−5158.

[12] G.E. De Benedetto, D. Fico, A. Pennetta, C. Malitesta, G. Nicolardi, D.D. Lofrument, F. De Nuccio, V. La Pesa, A rapid and simple method for the determination of 3,4-dihydroxyphenylacetic

acid, norepinephrine, dopamine, and serotonin in mouse brain homogenate by HPLC with fluorimetric detection, J. Pharm. Biomed. Anal. 98 (2014) 266-270.

[13] H.L. Cai, R.H. Zhu, H.D. Li, Determination of dansylated monoamine and amino acid neurotransmitters and their metabolites in human plasma by liquid chromatography-electrospray ionization tandem mass spectrometry, Anal. Biochem. 396 (2010) 103-111.

[14] K. Syslová, L. Rambousek, M. Kuzma, V. Najmanová, V.B. Valeˇsová, R. ˇSlamberová, P. Kaˇcer, Monitoring of dopamine and its metabolites in brain microdialysates: Method combining freeze-drying with liquid chromatography-tandem mass spectrometry, J. Chromatogr. A. 1218 (2011) 3382-3391.

[15] B. Kong, A. Zhu, Y. Luo, Y. Tian, Y. Yu, G. Shi, Sensitive and selective colorimetric visualization of cerebral dopamine based on double molecular recognition, Angew. Chem. Int. Ed. 50 (2011) 1837–1840.

[16] A. Chaicham, S. Sahasithiwat, T. Tuntulani, B. Tomapatanaget, Highly effective discrimination of catecholamine derivatives via FRET-on/off processes induced by the intermolecular assembly with two fluorescence sensors, Chem. Commun. 49 (2013) 9287-9289.

[17] M. Li, J.E. Zhu, L. Zhang, X. Chen, H. Zhang, F. Zhang, S. Xu, D.G. Evans, Facile synthesis of NiAl-layered double hydroxide/graphene hybrid with enhanced electrochemical properties for detection of dopamine, Nanoscale. 3 (2011) 4240–4246.

[18] H.B. Wang, H.D. Zhang, Y. Chen, K.J. Huang, Y.M. Liu, A label-free and ultrasensitive fluorescent sensor for dopamine detection based on double-stranded DNA templated copper nanoparticles, Sens. Actuators B Chem. 220 (2015) 146–153.

[19] W. Zhong, Nanomaterials in fluorescence-based biosensing, Anal. Bioanal Chem. 394 (2009) 47-59.

[20] M. Zhong, Y. Teng, S. Pang, L. Yan, X. Kan, Pyrrole-phenylboronic acid: A novel monomer for dopamine recognition and detection based on imprinted electrochemical sensor, Biosens. Bioelectron. 64 (2015) 212-218.

[21] B. Rezaei, M.K. Boroujeni, A.A. Ensafi, Fabrication of DNA, o-phenylenediamine, and gold nanoparticle bioimprinted polymer electrochemical sensor for the determination of dopamine, Biosens. Bioelectron. 66 (2015) 490-496.

[22] K. Jackowska, P. Krysinski, New trends in the electrochemical sensing of dopamine, Anal. Bioanal. Chem. 405 (2013) 3753–3771.

[23] Y. Xu, X. Hun, F. Liu, X. Wen, X. Luo, Aptamer biosensor for dopamine based on gold electrode modified with carbon nanoparticles and thionine labeled gold nanoparticles as probe, Microchim Acta. 182 (2015) 1797–1802.

[24] A.D. Ellington, J.W. Szostak, In vitro selection of RNA molecules that bind specific ligands, Nature. 346 (1990) 818–822.

[25] S. Tombelli, M. Minunni, M. Mascini, Analytical applications of aptamers, Biosens. Bioelectron. 20 (2005) 2424–2434.

[26] B.R. Baker, R.Y. Lai, M.S. Wood, E.H. Doctor, A.J. Heeger, and K.W. Plaxco, An electronic, aptamer-based small-molecule sensor for the rapid, label-free detection of cocaine in adulterated samples and biological fluid, J. A. Chem. Soc. 128 (2006) 3138-3139.

[27] H. Wei, B. Li, J. Li, E. Wang, S. Dong, Simple and sensitive aptamer-based colorimetric sensing of protein using unmodified gold nanoparticle probes, Chem. Commun. (2007) 3735–3737.

[28] H. Chang, L. Tang, Y. Wang, J. Jiang, and J. Li, Graphene fluorescence resonance energy transfer aptasensor for the thrombin detection, Anal. Chem. 82 (2010) 2341–2346.

[29] J.J. Li, X.Q. Zhong, H.Q. Zhang, X.C. Le, and J.J. Zhu, Binding-induced fluorescence turn-on assay using aptamer-functionalized silver nanocluster DNA probes, Anal. Chem. 84 (2012) 5170−5174.

[30] C. L. A. Hamula, J.W. Guthrie, H. Zhang, X.F. Li, X.C. Le, Selection and analytical applications of aptamers, Trends. Ana. Chem. 25 (2006) 681-691.

[31] Y.F. Huang, H.T. Chang, and W. Tan, Cancer cell targeting using multiple aptamers conjugated on nanorods, Anal. Chem. 80 (2008) 567-572.

[32] J. Zhou, W. Wang, P. Yu, E. Xiong, X. Zhang and J. Chen, A simple label-free electrochemical aptasensor for dopamine detection, RSC Adv. 4 (2014) 52250-52255.

[33] G.F. Gui, Y. Zhuo, Y.Q. Chai, Y. Xiang, and R. Yuan, In situ generation of self-enhanced luminophore by β-lactamase catalysis for highly sensitive electrochemiluminescent aptasensor, Anal. Chem. 86 (2014) 5873−5880.

[34] C. Wu, L. Du, L. Zou, L. Huang, P. Wang, A biomimetic bitter receptor-based biosensor with high efficiency immobilization and purification using self-assembled aptamers, Analyst. 138 (2013) 5989-5994.

[35] H.J. Kim, C.H. Jang, Liquid crystal-based aptasensor for the detection of interferon-γ and its application in the diagnosis of tuberculosis using human blood, Sens. Actuators B Chem. 282 (2019) 574–579.

[36] H. Ren, Z. An, C.H. Jang, Liquid crystal-based aptamer sensor for sensitive detection of bisphenol A, Microchemical Journal. 146 (2019) 1064–1071.

[37] J.M. Brake, M.K. Daschner, Y.Y. Luk, N.L. Abbott, Biomolecular interactions at phospholipid-decorated surfaces of liquid crystals, Science. 302 (2003) 2094–2097.

[38] J.M. Brake, N.L. Abbott, Coupling of the orientations of thermotropic liquid crystals to protein binding events at lipid-decorated interfaces, Langmuir. 23 (2007) 8497–8507.

[39] S.J. Woltman, G.D. Jay, G.P. Crawford, Liquid-crystal materials find a new order in biomedical applications, Nat. Mater. 6 (2007) 929–938.

[40] H. Kim, Z. An, C.H. Jang, Label-free optical detection of thrombin using a liquid crystal-based aptasensor, Microchemical Journal. 141 (2018) 71–79.

[41] S. Yang, C. Wu, H. Tan, Y. Wu, S. Liao, Z. Wu, G. Shen, and R. Yu, Label-free liquid crystal biosensor based on specific oligonucleotide probes for heavy metal ions, Anal. Chem. 85 (2013) 14-18.

[42] S. Deng, Q. Jiang, T. Zhang, X. Xiong, P. Chen, Liquid crystal biosensor based on Cd^{2+} inducing the bending of PS-oligo for the detection of cadmium, Health. 7 (2015) 986-993.

[43] C. Mannironi, A.D. Nardo, P. Fruscoloni, and G.P. Tocchini-Valentini, *In vitro* selection of dopamine RNA ligands, Biochemistry. 36 (1997) 9726-9734.

[44] X. Su, W. Huo, D. Yang, C. Luan, J. Xu, Label-free liquid crystal immunosensor for detection of HBD-2, Talanta. 203 (2019) 203–209.

[45] G.M. Koenig, Jr.R. Ong, A.D. Cortes, J.A. Moreno-Razo, J.J. de Pablo, N.L. Abbott, Single nanoparticle tracking reveals influence of chemical functionality of nanoparticles on local ordering of liquid crystals and nanoparticle diffusion coefficients, Nano Lett. 9 (2009) 2794–2801.

[46] R. Nandi, L. Loitongbam, J. De, V. Jain and S.K. Pal, Gold nanoparticle-mediated signal amplification of liquid crystal biosensors for dopamine, Analyst. 144 (2019) 1110-1114.

[47] R. Walsh, M.C. DeRosa, Retention of function in the DNA homolog of the RNA dopamine aptamer, Biochemical and Biophysical Research Communications. 388 (2009) 732–735.

Highlights

- A novel optical liquid crystal-based aptasensor using dopamine-binding DNA aptamers as recognition elements was developed for the detection of dopamine.
- The aptasensor displayed a wide linear range of 1 pM to 10 µM (0.19 pg/mL to 1.9 µg/mL) and a very low detection limit of 10 pM (~1.9 pg/mL) towards dopamine.
- The liquid crystal-based aptasensor showed high selectivity for dopamine detection.

Author contributions- CRediT

Duy Khiem Nguyen: Conceptualization, Methodology, Data curation, Writing-Original draft, Writing-Reviewing and Editing, Visualization, Investigation

Chang-Hyun Jang: Conceptualization, Methodology, Funding acquisition, Supervision.